photonics

MDPI

Article

High-Speed Underwater Optical Wireless Communication with Advanced Signal Processing Methods Survey

Chengwei Fang [1,*], Shuo Li [1], Yinong Wang [2] and Ke Wang [1]

[1] School of Engineering, Royal Melbourne Institute of Technology (RMIT) University, Melbourne, VIC 3000, Australia; shuo.li2@rmit.edu.au (S.L.); ke.wang@rmit.edu.au (K.W.)
[2] School of Architecture and Urban Design, Royal Melbourne Institute of Technology (RMIT) University, Melbourne, VIC 3000, Australia; s3576616@student.rmit.edu.au
* Correspondence: s3643273@student.rmit.edu.au

Abstract: Underwater wireless communication (UWC) technology has attracted widespread attention in the past few years. Compared with conventional acoustic underwater wireless communication technology, underwater optical wireless communication (UOWC) technology has promising potential to provide high data rate wireless connections due to the large license-free bandwidth. Building a high-performance and reliable UOWC system has become the target of researchers and various advanced and innovative technologies have been proposed and investigated. Among them, better hardware such as transmitters and receivers, as well as more advanced modulation and signal processing techniques, are key factors in improving UOWC system performance. In this paper, we review the recent development in UOWC systems. In particular, we provide a brief introduction to different types of UOWC systems based on channel configuration, and we focus on various recent studies on advanced signal processing methods in UOWC systems, including both traditional non-machine learning (NML) equalizers and machine learning (ML) schemes based on neural networks. In addition, we also discuss the key challenges in UOWC systems for future applications.

Keywords: underwater optical wireless communication (UOWC); digital signal; linear equalizer; nonlinear equalizer; supervised machine learning; reinforcement machine learning

Citation: Fang, C.; Li, S.; Wang, Y.; Wang, K. High-Speed Underwater Optical Wireless Communication with Advanced Signal Processing Methods Survey. *Photonics* **2023**, *10*, 811. https://doi.org/10.3390/photonics10070811

Received: 31 May 2023
Revised: 4 July 2023
Accepted: 10 July 2023
Published: 12 July 2023

1. Introduction

The ocean covers more than 70 percent of the surface of our planet [1]. Human exploration of the ocean has not stopped since ancient times. With the rapid development of science and technology, human exploration of the ocean has gradually deepened. The invention and optimization of a large range of underwater applications such as underwater wireless sensor networks [2] and autonomous underwater vehicles (AUVs) [3] have become key factors. Underwater wireless communication (UWC) technologies, which are summarized in Table 1, have become the cornerstone of these underwater applications. With the need for real-time underwater communications, high-speed and long-distance transmission is more in demand than ever in UWC technologies.

Traditional UWC mainly relies on underwater acoustic communication (UAC) technology, which has been explored in transmitting data for long distances reaching up to several tens of kilometers [4], exploring the low attenuation property enabled by the physical properties of sound waves propagating in water. However, UAC suffers from a low data rate limitation due to the low modulation bandwidth (only tens of kHz) [5,6]. The propagation speed of acoustic waves in the underwater channel is also low (only 1500 m/s), leading to a latency of about 0.67 s per kilometer [7]. Moreover, the power consumption is typically high (tens of watts [8]). Compared to UAC, underwater radio frequency (RF) communication suffers from a high attenuation coefficient due to the low conductivity of electromagnetic waves in water, which leads to a highly limited transmission distance (only a few meters to tens of meters) [9]. Thus, RF communication is not adopted in UWC.

To overcome the conventional UWC limitations, UOWC has been proposed and widely studied since it has great potential to achieve a higher data rate reaching Gbps, thanks to the large modulation bandwidth (exceeding MHz [10] and even GHz [11], typically limited by the transceiver). Moreover, the physical communication latency is much shorter due to the high propagation speed of light in the underwater channel [12]. These high-speed and low-latency advantages can enable many real-time applications. Furthermore, UOWC is also cost-effective and power-effective compared to UAC and RF communication, which benefits from low-cost and low-power transceivers such as light-emitting diodes (LEDs) and photodiodes (PDs) [13]. Although the UOWC technology has these advantages, the transmittance of the optical wave is limited compared with the acoustic wave (only hundreds of meters in the tap water channel [14]), and due to the shorter wavelength, the optical signal also experiences more complex underwater propagation channels. Hence, improving the transmission distance, data rate, and system stability of the UOWC system becomes a research focus.

Table 1. Comparisons of three underwater wireless communication technologies.

	Acoustic Systems	**Radio Frequency Systems**	**Optical Wireless Systems**
Attenuation	Low	High	Moderate
Distance	Long (tens of kilometers)	Short (tens of meters)	Limited (hundreds of meters)
Carrier Frequency	Low (10 Hz–1 MHz)	Moderate (30 Hz–300 MHz)	High (10^{12} Hz–10^{15} Hz)
Bandwidth	Narrow (kHz)	Moderate (MHz)	Broad (MHz–GHz)
Data Rate	Low (kbps)	Moderate (Mbps)	High (Gbps)
Power Consumption	High	High	Low
Transmission Latency	High (1500 m/s physical propagation speed of sound wave)	Low (2.26×10^8 m/s physical propagation speed of electromagnetic wave)	Low (2.26×10^8 m/s physical propagation speed of optical wave)
Performance-limiting factors	Temperature, hydrostatic pressure, and the chemistry of water	Conductivity and permitivity	Absorption, scattering, turbidity, marine life blocking, and beam shaping

In recent years, a number of surveys and summary papers on UOWC have been published, which are summarized in Table 2. In [8,15–18], brief overviews and recent advances of UOWC are presented, focusing on the UOWC channel characterization, modulation methods, and coding technologies. In addition to an overview of recent UOWC achievement, in [19], a summary of transmitter and receiver technologies is presented. Moreover, the UOWC channel model and the impact of underwater turbulence are discussed. Due to the complex underwater environment, accurate theoretical UOWC channel models are the basis for designing and optimizing practical UOWC systems. Therefore, the available UOWC models to investigate the communication performance, such as the transmission range and data rate, are summarized in [20,21]. With the continuous optimization and improvement of theoretical models, many practical UOWC systems have been further designed and studied experimentally. In [13], a detailed summary of UOWC experimental demonstrations with both laser diode (LD) and LED transmitters in recent years is presented. In addition, some key technologies, such as higher sensitivity receivers and more advanced signal modulation methods are also presented to improve the transmission capacity and performance of UOWC systems.

In addition, some recent survey papers also provide a more focused review of key parts of the UOWC system, such as the network layer and underwater channel turbulence. In [2], in addition to the physical layer such as the channel characterization and modulation methods, the network layer issues, including the link configuration and budgets, multiple access schemes, relaying techniques, and potential routing algorithms are also presented. In addition to the absorption and scattering of the signal beam by the particles in the water, UOWC systems also face great challenges from underwater optical turbulence (UOT), which is physically caused by the fluctuation of water with random variations of temperature and pressure [22]. In [23], theoretical UOWC system models considering

turbulent channels are summarized, together with underwater turbulence mitigation technologies in the physical layer, including aperture averaging, optical beam shaping, transmitter and receiver enhancement, and multiple-input multiple-output (MIMO) spatial diversity techniques.

With the rapid development of UOWC technologies, increasingly more UOWC applications have begun to appear, which are captured by a few recent survey papers. For instance, in [24], the UOWC-based Internet of Underwater Things (IoUT) network is summarized, focusing on the medium access control (MAC) aspect. Moreover, AUVs, which are key technologies for the maritime industry are widely deployed for commercial, scientific, environmental, and defense applications. Thanks to high-speed data transmission, the UOWC technology has been widely considered in AUV application. In [3], a summary of swarm robotics techniques based on the LED type of UOWC is presented.

Through the above literature review, due to the absorption and scattering of signal light caused by the complex underwater environment and the influence of underwater turbulence on channel stability, UOWC faces challenges of limited transmission distance and fluctuating transmission reliability [23]. In order to improve the transmission distance of UOWC and to achieve more stable system performance, a large number of techniques have been studied in the physical layer [8,15–19], such as more advanced transmitter technologies (e.g., high-bandwidth Gallium nitride (GaN)-based mini-LEDs [25], two-stage-injection-locked technique [26,27]), more sensitive receiver technologies (e.g., lensed array optical interface [28,29], photomultiplier tubes (PMT) [30], and single-photon avalanche diode (SPAD) [31]), and more advanced UOWC spatial technologies (MIMO principles [32–34]). The signal processing enhancement, which includes transmitter frequency response improvement [27,29,35], transmitter shot noise minimization [36], and inter-symbol interference (ISI) elimination techniques [28,37,38], has also achieved remarkable progress in recent years. Digital signal processing (DSP) technologies can significantly improve the signal-to-noise ratio (SNR) and reduce the bit-error rate (BER) of UOWC systems with low cost and high efficiency.

Although the previous survey papers [2,13] included the DSP aspect, only a short and simple introduction is presented. Therefore, this survey provides a comprehensive review of the recent developments of advanced DSP techniques in UOWC systems, which include:

1. A brief introduction and summary of equalization principles.
2. A detailed review of NML equalization techniques in UOWC systems in recent years, including both linear equalizers and nonlinear equalizers.
3. A detailed review of ML techniques in UOWC systems, including both supervised learning and reinforcement learning schemes.

The rest of this survey is organized as follows: in Section 2, we introduce the general architecture and principles of UOWC systems. Moreover, we discuss and summarize equalization technique principles and introduce ML applications in UOWC systems. In Section 3, we provide a detailed review of the linear equalizers and nonlinear equalizers applied in recent UOWC progress. In Section 4, we provide a review of ML applications in UOWC. Moreover, we discuss the challenges of both NML and ML equalizers and provide our views on future UOWC technologies from the advanced signal processing techniques perspective in Section 5. Finally, we conclude the survey in Section 6.

Table 2. Recent surveys and the comparison with this paper.

References	Year	Area of Focus
Hemani Kaushal et al. [8]	2016	• UOWC LOS, NLOS, and retro-reflector channels • Optical attenuation modeling • UOWC system design • Future scope
Zhaoquan Zeng et al. [15]	2017	• UOWC LOS and NLOS channels • Optical attenuation and turbulence modeling • Theoretical modulation and coding • Practical implementations of UOWC
Hassan M. Oubei et al. [19]	2018	• UOWC typical LOS and NLOS channels • Optical attenuation and turbulence modeling • Future challenge in transceiver technologies
Callum T. Geldard et al. [20]	2019	• UOWC absorption and scattering modeling • Monte Carlo simulation discussion
N. E. Miroshnikova et al. [21]	2019	• UOWC LOS and NLOS channels • Optical absorption and scattering modeling
Nasir Saeed et al. [2]	2019	• UOWC potential channel architectures • Layer-by-layer network aspects • Localization • Future scope discussion
T. R. Murgod et al. [16]	2019	• UOWC network architecture • Routing and localization algorithms introduction • Recent related work challenges discussion
Chuyen T. Nguyen et al. [24]	2020	• UOWC-based Internet of Underwater Things network • Physical and MAC cross-layer analysis • Monte Carlo simulation analysis
G. S. Spagnolo et al. [17]	2020	• UOWC optical attenuation modeling • UOWC transceiver technologies
Shijie Zhu et al. [13]	2020	• UOWC recent theoretical summary • Recent experimental progress summary • Advanced modulation techniques • Challenges and perspectives
SAH Mohsan et al. [18]	2020	• UOWC recent progress • Optical scattering and absorption challenges • Modulation technologies and channel coding
PA Hoeher et al. [3]	2021	• UOWC in swarm robotics • Channel modeling fundamental • Physical layer transmission techniques • Data link layer aspects • Interference suppression • Realization aspects
Y. Baykal et al. [23]	2022	• UOWC turbulence modeling • Turbulence mitigation techniques
This survey	2023	• UOWC fundamental overview • Introduction of equalization principles • Recent UOWC work based on NML equalization • Recent ML equalization techniques in UOWC systems • DSP challenge discussions

2. Overview of UOWC Systems

2.1. System Architecture

Before introducing the typical UOWC system, it is essential to provide an overview of the UOWC network architecture. As shown in Figure 1, AUVs can use the UOWC system to communicate with divers and optical base stations (OBSs) in real time. Moreover, the underwater monitor (UM) can use underwater cameras to transmit real-time video signals through UOWC techniques to OBSs and finally to relevant departments to monitor water quality and deter poachers. Furthermore, the underwater defense system can use UOWC sensor technologies to detect enemies in time and take a counter measurement. At the same time, OBSs connect with the central OBS on the water surface to form a complete underwater sensor network. The central OBS can further communicate with satellites and ships by the RF link, truly realizing the integrated underwater-above-water-satellite communication network.

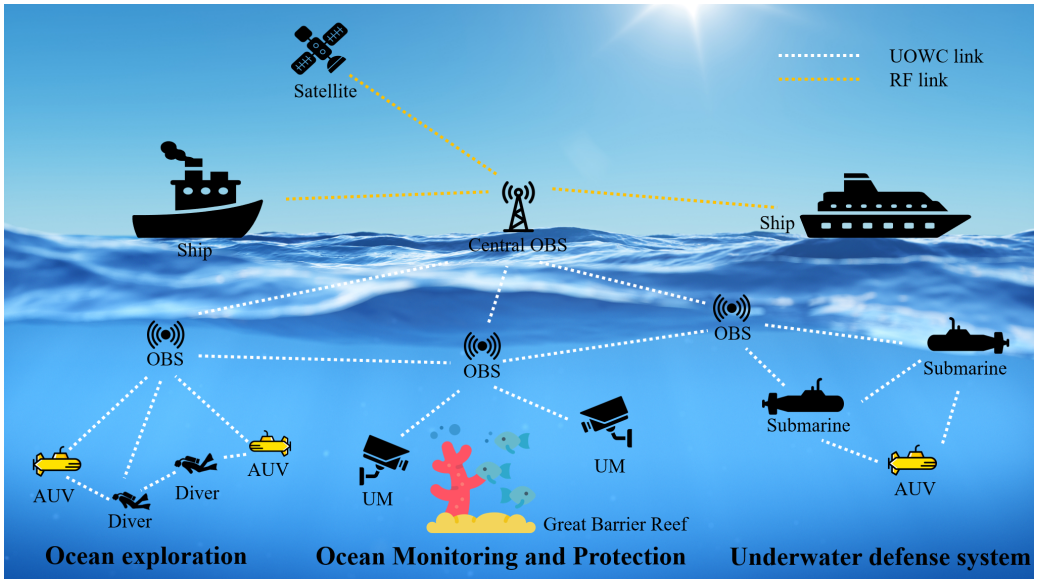

Figure 1. UOWC network architecture.

The typical UOWC system, which includes the transmitter, the medium, and the receiver, is shown in Figure 2. In the transmitter part, the signal is generated and mapped to transmitted symbols before being loaded into a digital-to-analog converter (DAC). The most widely used symbol modulation techniques used are on–off keying (OOK) [39–43] and pulse position modulation (PPM) [44–47]. OOK is the simplest modulation method and is widely used together with direct detection. However, the OOK modulation is susceptible to interference in the complex underwater environment [8,13]. PPM is beneficial for long-distance UOWC communication since it is more power efficient. However, the PPM suffers from the disadvantage of low spectral efficiency. To achieve a high data rate transmission, more advanced signal modulation methods, such as multi-level pulse amplitude modulation (PAM) [27,35,48–50] and quadrature amplitude modulation (QAM) [51–55], have been applied in recent studies. PAM uses multiple power levels to modulate information, and hence, provides higher spectral efficiency. However, due to PAM requiring a higher SNR for correct symbol detection, the power consumption is high. Furthermore, QAM further improves the data rate by exploring quadrature features. However, due to its high implementation complexity, QAM modulation has high cost limitations [15].

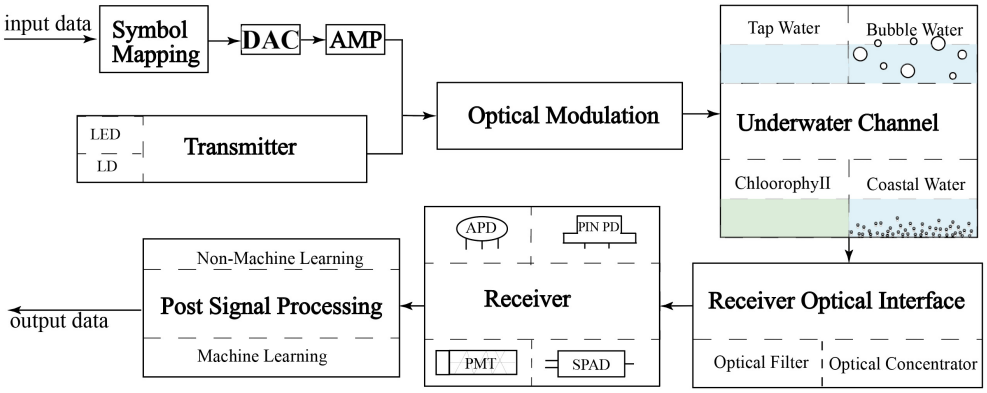

Figure 2. General architecture of UOWC system.

After symbol mapping, the digital signal is loaded into a DAC. After amplification (AMP), the signal is then modulated to the optical carrier. There are two optical transmitters that are widely used in UOWC. The first one is LED, which has the advantages of a wide optical beam and low cost. Hence, the LED-based UOWC system is widely used in short-range applications with a large signal coverage area (tens of meters transmission distance [10,41,49,56]). However, the modulation bandwidth is typically limited to tens of MHz [10,57] or hundreds of MHz [58], restricting the transmission data rate [54,58]. Compared with LED, the LD transmitter has the advantage of broad modulation bandwidth over the GHz range [11,27,59–61]. Hence, the transmission data rate of LD-based UOWC systems can reach tens of Gpbs [27,52,53,62]. Moreover, the narrow laser beam also enables a longer link distance of hundreds of meters [38]. However, due to the narrow laser beam, the transmission performance degrades sharply by underwater scattering and turbulence [8]. In addition, LD transmitters also have a higher cost compared to LEDs.

To modulate symbols to the optical carriers, two methods are widely used. The most common method in UOWC systems is direct modulation, which uses a bias tee to combine the electrical signal generated by the DAC with the DC bias, which is then connected to the optical transmitter [30,63,64]. The advantage of direct optical modulation is simple and efficient. However, the modulation bandwidth is limited and is only capable of intensity modulation. To overcome these limitations, external optical modulation methods can be used; the Mach–Zehnder Modulator is widely employed in LD-based UOWC systems [65–67].

After signal generation, the optical beam propagates through the underwater channel. The two main physical phenomenons that cause signal loss in the underwater channel are absorption and scattering, as shown in Figure 3. When the optical beam with optical power P_i at a wavelength λ propagates in the water, a small part is absorbed, denoted by P_a, and another part is scattered, denoted by P_s. The remaining part P_t reaches the receiver [8]. Generally, the attenuation coefficient $c(\lambda)$ is the sum of absorption coefficient $a(\lambda)$ and scattering coefficient $b(\lambda)$ [68]:

$$c(\lambda) = a(\lambda) + b(\lambda). \tag{1}$$

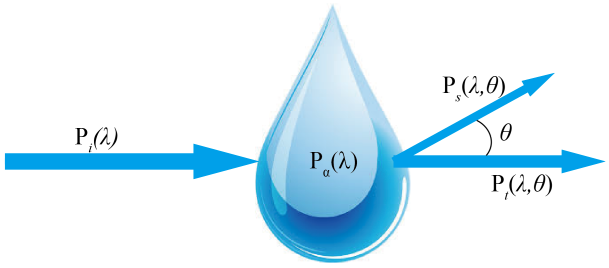

Figure 3. Geometry of optical beam propagation underwater.

The propagation path loss L_p, as a function of wavelength λ and distance d, is then given as [69]

$$L_p(\lambda, d) = e^{-c(\lambda)d}. \quad (2)$$

The attenuation coefficient $c(\lambda)$ is highly dependent on the optical wavelength [70], where the range of 450–550 nm (blue and green lights) has a much smaller attenuation coefficient compared to other wavelengths. Hence, the blue and green wavelength bands are typically used in UOWC systems. Another factor that affects the attenuation coefficient is the type of water. Since the UOWC technology is typically applied in the ocean, the attenuation coefficient of seawater has become a key research focus. In [71], it was found that the absorption coefficient $a(\lambda)$ is determined by organic pigments (chlorophyll, carotenoids, pheophytin, and chlorophyllide) produced by aquatic plants in water, and the scattering coefficient $b(\lambda)$ is dependent on the density and volume of particles in water. However, ocean water at different depths and locations has differences in sunlight strength and temperature, causing differences in the organic pigment levels and the density and volume of particles. Therefore, in previous studies, the water channel is typically divided into three categories: clear ocean, coastal ocean, and turbid harbor. The typical values of absorption and scattering coefficients of the three different ocean water types are concluded in Table 3 [8].

Table 3. Typical values of absorption and scattering coefficients in three different ocean water types.

Ocean Water Type	a (m^{-1})	b (m^{-1})	c (m^{-1})
Clear ocean	0.114	0.037	0.151
Coastal ocean	0.179	0.220	0.339
Turbid harbor	0.366	1.829	2.195

In UOWC experiments, many researchers use tap water with a lower attenuation coefficient ($c \approx 0.07$ m^{-1}) [26,27,72]. To achieve experimental results closer to practical systems, the chlorophyll base of a seawater channel was investigated in recent UOWC studies [73–75]. As a very common phenomenon in water, bubbles will also affect the performance of UOWC systems. There have been some recent studies investigating UOWC bubble channels [76–78]. In addition, near the ocean surface and harbor, coastal ocean water and turbid harbor water channels have always been a huge challenge for UOWC communications since these two kinds of water often have high levels of organic pigments and particles, leading to a large attenuation coefficient [8,13]. In recent years, there has been research focusing on the improvement in coastal and turbid harbor water channels [35,60,79].

After passing through the underwater channel, an optical interface is typically used at the receiver to reduce the impact of the background light (sunlight) and to focus signal light, such as optical filters to suppress the background light [80–82], and the lens array to collect more signal light [28,29]. Then, the signal light is detected by the optical detector. The PIN photodiode (PIN PD), which has the advantages of fast response time, low cost, and good tolerance to ambient light [8], is widely employed [10,50,51,53–56,58–60,62,83–85]. The avalanche photodiode (APD) has also been utilized due to the higher internal gain [10,28,35,38,41,42,49,52,64,86–89]. However, APDs also require high bias voltage, complex control circuitry, and are more sensitive to ambient noise.

Due to the relatively high path loss, UOWC systems require a sensitive receiver to increase the transmission distance. Hence, PMT has been explored, which has a high gain, low noise, and a large collection area [8]. Moreover, SPAD, which operates at a reverse voltage higher than the breakdown voltage to further increase the internal gain and sensitivity, has also been investigated [13]. With PMT and SPAD, a 50 m UOWC link with 500 kbps data rate and 117 m UOWC link with 2 Mbps data rate have been demonstrated [14,90].

In UOWC systems, both the line-of-sight (LOS) link and non-line-of-sight (NLOS) link have been studied, as shown in Figure 4. Direct LOS link is the most simple link configuration and has been widely studied both theoretically and experimentally [82,91].

However, in practical underwater environments, marine life and reefs can block the channel. To overcome this limitation, NLOS-based UOWC systems, which use the water–air surface or bubbles underwater to reflect the signal to avoid obstacles, are investigated in recent studies [80,92,93], including a few NLOS UOWC experimental demonstrations [46,94]. Moreover, the NLOS link configuration is also applied in highly turbid water to achieve a high transmission data rate and bypass obstacles [95,96].

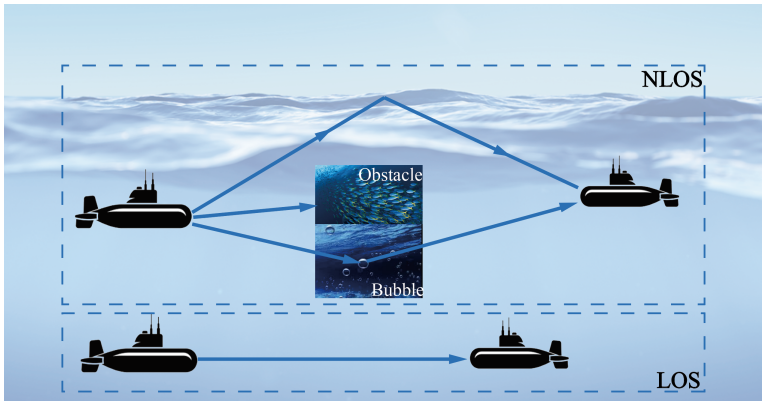

Figure 4. UOWC channel configurations.

2.2. Signal Processing Techniques

As mentioned in Figure 3, when light passes through water, some of the light is scattered and travels in other directions. Generally, the Henyey–Greenstein (HG) function and the two-term Henyey–Greenstein (TTHG) function [97] are widely used to represent the scattering phase function (SPF) in UOWC systems [8,98], which are widely used in the Monte Carlo (MC) simulation of UOWC systems [80,99–102]. Due to the scattering in the underwater channel, the signal photons arrive at the detector through different optical paths, leading to a delay in the time-of-arrival and ISI, which degrades the signal quality and reduces the transmission data rate. Since scattering is determined by the size and density of particles in water, ISI has little impact on deep sea or clear ocean UOWC systems. However, in harbor water and coastal water, the performance of UOWC systems is highly affected by ISI [8,39,103].

In most practical UOWC applications, eliminating the ISI at the receiver is not trivial because the channel response is not accurately known. The simplest and most common signal-processing technique to suppress the impact of ISI is the linear equalizer. Among them, zero-forcing linear equalizer (ZF-LE), which equalizes the folded spectrum of the received signal using a filter with the inverse frequency response, has been applied in many UOWC studies [37,104,105]. The ZF-LE can eliminate the ISI at the sampling time to increase the system SNR. However, the ZF-LE cannot be used when the folded spectrum has nulls, which can cause infinite noise enhancement. To avoid this, the mean-square error linear equalizer (MSE-LE) has been studied. Unlike the ZF-LE eliminating the ISI, the MSE-LE passes a small part of ISI to the output to improve the SNR and BER in UOWC systems [31,106]. It needs to be mentioned that we only give a snapshot here and more details of these works are presented later.

Even though linear equalizers are easy to operate in systems, the infinite noise enhancement of ZF-LE with spectral nulls and large noise enhancement of MSE-LE with deep attenuation in the passband limit their applications. To overcome these issues, more complex and advanced nonlinear equalizers have been further studied in UOWC systems. One of the most common nonlinear equalizers in UOWC systems is the zero-forcing decision-feedback equalizer (ZF-DFE), which is designed to cancel ISI and completely avoid infinite noise enhancement by employing a whitened matched filter. To further improve the performance, the mean-square error decision-feedback equalizer (MSE-DFE) was investigated, which uses a linear predictor and a feedback filter to whiten the noise at the output. Due to its complex structure and design, MSE-DFE is rarely used in UOWC systems but is

widely used in UAC systems [107–109]. In summary, signal processing techniques that rely on non-machine learning equalizers are widely used in UOWC systems. In Section 3, we review the recent studies of non-machine learning equalization in UOWC systems.

With the development of neural networks and artificial intelligence, ML applications based on neural networks have been widely investigated in UOWC systems to enhance performance. In general, there are four types of machine learning algorithms: supervised, unsupervised, semi-supervised, and reinforcement learning. The most commonly used ML algorithm in the UOWC system is supervised learning, which uses known output features to derive computational relationships between input training data and output data [110]. The supervised ML method has been widely applied in signal processing to suppress various impairments in the UOWC system, such as improve the BER and enhance stability [50,111–115]. The encoder/decoder based on supervised ML algorithms has also been studied to improve the data transmission in recent UOWC research [116,117].

Another ML algorithm explored in the UOWC system is reinforcement learning, which focuses on developing an optimized strategy by monitoring how an intelligent agent acts in an environment to maximize cumulative reward. The reinforcement learning method has been applied to improve the communication stability [118–120] and to reduce the power consumption and improve link quality via optimizing the routing protocol in an underwater sensor network [121,122]. In Section 4, we provide a comprehensive survey on the recent UOWC progress based on ML algorithms.

3. Non-Machine Learning Equalization

3.1. Linear Equalizer

UOWC has developed rapidly in recent years and made remarkable achievements. Table 4 lists the recent studies of NML linear equalization in UOWC systems.

Table 4. Research progress in the UOWC system based on NML linear equalization.

Year	Bit Rate (bps)	Distance	Optical Source	Receiver	Transmission Power	Modulation Scheme	Equalizer	Refs.
2013	1 G	40 m Coastal	532 nm LED	PD	∼50 W	OOK	ZF-LE	[37]
2017	1 M	3 m Tap	532 nm LED	SPAD	N/A	OFDM-QAM	MMSE-FDE	[31]
2019	256 G	50 m Air 5 m Turbid	Red LD	APD	∼500 W	PAM4	FDE	[79]
2019	30 G	12.5 m Tap 2.5 m Harb	488 nm LD	APD	∼20 mW	PAM4	FDE	[35]
2020	20 M 50 M	28 m Tap 10 m Tap	470 nm LED	SiPM	∼600 mW	PAM	FDE	[123]
2020	3.31 G	56 m Tap	520 nm LD	APD	∼50 mW	OFDM	FDE-NP	[63]
2021	1 G	1 m Tap	377 nm LD 405 nm LD	2APDs	∼70 mW to 120 mW	NRZ-OOK	ZF-LE	[104]
2022	4 G	2 m Tap	484 nm LED	APD	∼1 mW	PAM4	FFE	[25]

Due to simplicity and efficiency, the linear ZF-LE and feedforward equalizer (FFE) have been studied in UOWC systems to enhance data transmission performance. In [37], to reduce the effect of ISI and improve the BER, the ZF-LE based on the double Gamma model was employed in a UOWC system with coastal water. MC results show that to achieve the forward error correction (FEC) threshold (3.8×10^{-3}), the ZF-LE can reduce the transmission power by around 2 dBm and 1.5 dBm in the 1 Gbps 40 m coastal water link and the 500 Mbps 10 m harbor water link, respectively. In addition, the ZF-LE combined with the dual-wavelength UOWC transmission was demonstrated in [104] to improve the BER simultaneously in two wavelength channels. Results in Figure 5 show that the ZF-LE can restore eye opening in the corresponding eye diagram of both blue and green channels and improve the BER performance. Furthermore, a linear T/2-spaced feedforward equalizer (FFE) combined with the high-bandwidth GaN-based mini-LEDs was demonstrated in [25]. Due to mitigating the ISI by simple and efficient FFE, the net

data rate can reach up to 4.08 Gbps (the highest for UOWC systems using a single-pixel mini-LED) with a BER below the FEC threshold in short-distance transmission.

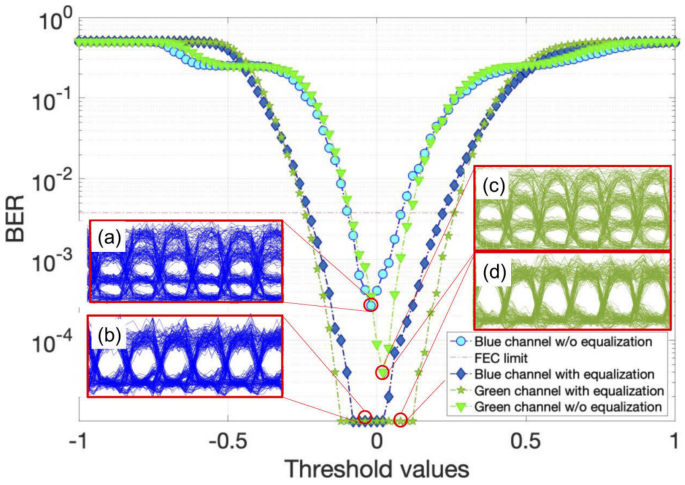

Figure 5. Bathtub curve for blue and green channels using 377- and 405-nm transmitters with and without ZF-LE [104].

In addition to the simple ZF-LE, low-complexity linear frequency domain equalizers (FDE) were also employed to mitigate the ISI effect. In [123], the FDE combined with high sensitive silicon photo-multipliers (SiPMs) receiver was employed to overcome the limited bandwidth of components at a high data rate. Results show that the FDE can significantly improve BER from 1×10^{-1} to 0.9×10^{-4} in a 10 Mbps UOWC system with a 40 m tap water channel. Moreover, the FDE can improve the data rate to achieve 20 Mbps and 50 Mbps transmission under 28 m and 10 m tap water channels, respectively. In addition, linear FDE has also been studied in the free-space optical underwater optical wireless communication (FSO-UOWC) convergent system to optimize the modulation frequency response and enhance the transmission capacity [79]. Together with the two-stage injection locking technique, a 256 Gb/s four-channel FSO-UOWC convergent system with 50 m free space and 5 m turbid underwater transmission is successfully demonstrated. Furthermore, in another work [35], a red LD is used as the transmitter, and both an injection-locking optoelectronic feedback and a linear FDE at the receiving end are applied. Results show that the 3 dB bandwidth can be increased from 8.4 GHz to 10.8 GHz using the linear FDE. The linear FDE has also been utilized to compensate for the frequency response (especially for high frequencies) to enhance the transmission rate of a PAM4 UOWC system. Results show that under both a 12.5 m piped underwater channel and a 2.5 m high-turbidity harbor underwater channel, 30 Gbps transmission can be achieved.

However, due to the limited capability of the conventional FDE when the folded spectrum has nulls, a one-tap minimum mean square error (MMSE) FDE was employed in [31]. Results show that the MMSE-FDE can significantly reduce the noise enhancement in frequency-selective channels with spectral nulls of the coded UOWC systems, which further improves the BER performance by 2 to 4 dB for three water types. In addition to the MMSE, the conventional linear FDE can also be combined with noise prediction (NP) shown in Figure 6 to better mitigate the impact of ISI [63]. Results show that the SNR required to achieve the same BER can be reduced by 3.8 dB using the proposed FDE-NP scheme compared with the conventional FDE. Due to the efficient equalization by FDE-NP, a maximum net data rate of 3.48 Gbps is achieved, which is about 17.2% higher than the traditional OFDM UOWC system. Furthermore, a 56 m UOWC system with a data rate of 3.31 Gbps is demonstrated with FDE-NP.

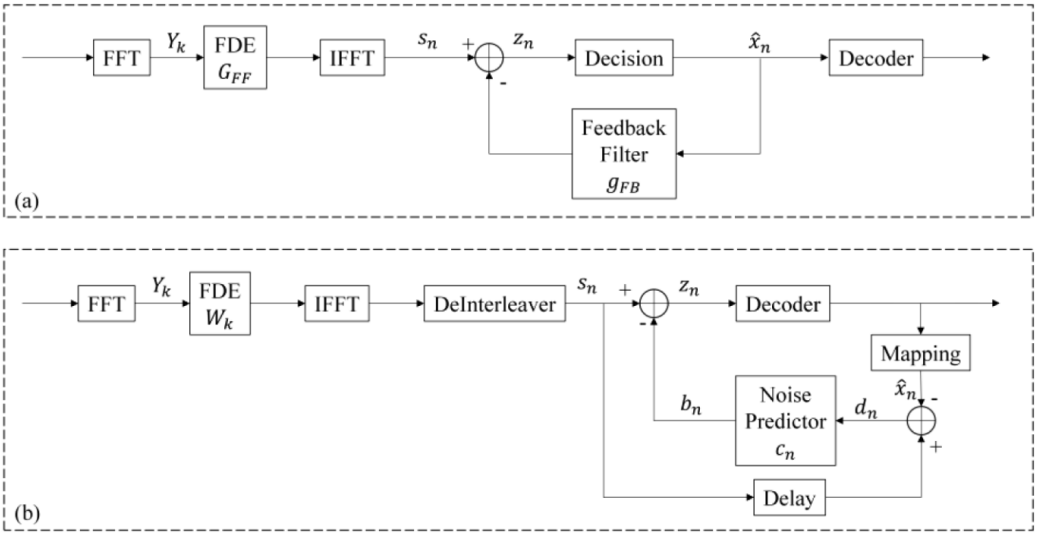

Figure 6. The receiver structure of the (**a**) FDE-DFE, (**b**) FDE-NP [63].

3.2. Nonlinear Equalizer

Compared with the linear equalizer, the nonlinear equalizer has a more complex structure but superior ISI mitigation performance. It is also widely used in the recent UOWC systems, which are summarized in Table 5.

Table 5. Recent research progress in UOWC systems based on NML nonlinear equalization.

Year	Bit Rate (bps)	Distance	Optical Source	Receiver	Transmission Power	Modulation Scheme	Equalizer	Refs.
2016	9.6 G	8 m Tap	405 nm LD	PD	~30 mW	16-QAM-OFDM	TPGE	[26]
2016	745 M	2 m Tap	448 nm LED	APD	~184.5 mW	OFDM-QAM	APE	[124]
2017	16 G	10 m Tap	488 nm LD	PD	~20 mW	PAM4	DFE	[27]
2018	16.6 G	55 m Tap	450 nm LD	PIN PD	~120 mW	OFDM-QAM	VE	[62]
2018	7.33 G	15 m Tap	450 nm LD	APD	~20 mW	DMT	VE	[64]
2019	2.5 G	60 m Tap	450 nm LD	APD	~50.2 mW	NRZ-OOK	VE	[28]
2019	500 M	100 m Tap	520 nm LD	APD	~7.25 mW	NRZ-OOK	VE	[38]
2019	500 M	1 m Bubble	520 nm LD	APD	~25 mW	16PPM	VE	[76]
2021	200 M	100 m Tap	450 nm LD 520 nm LD	PMT	~700 mW	RRC-OOK	MPE	[30]
2022	4.12 G	2 m Tap	484 nm LED	APD	~ 1 mW	PAM4	VE	[125]
2022	200 M	1.5 m Tap	Blue LED	PD	~0.4 mW	CAP OFDM	VDFE	[126]

Earlier, many UOWC experiments used an analog equalizer to improve the system frequency response. In [26], a physical tunable passive gain equalizer (TPGE) combined with the two-stage-injection-locked technique was employed to improve the frequency response, as shown in Figure 7. The frequency response of the signal is compensated by around 10 dB after TPGE, where the electrical spectrum of the data signal after TPGE is flatter, improving the system transmission performance. Results show that BER can be improved from 2×10^{-2} to 4×10^{-2} in an 8 m tap water channel under a transmission speed of 9.6 Gbps. Similarly, in [124], an analog post-equalizer(APE) was demonstrated to increase the 3 dB frequency response of the system from 4 MHz (LED) and 100 MHz (detector) to 124.2 MHz end-to-end. Due to the broader and flatter 3 dB bandwidth of the system, high spectral efficiency modulation formats such as OFDM can be applied. Results show that the SNR increased from 8.75 dB to 22.6 dB after employing the APE. Moreover, the BER improved from 1.2×10^{-1} to 3.9×10^{-4} in a UOWC link at 621.1 Mbps with 2 m tap water.

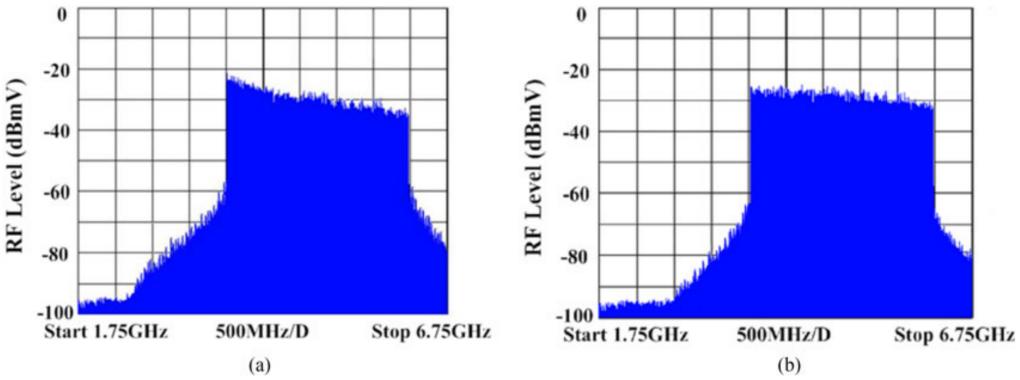

Figure 7. Electrical spectra of the 9.6 Gbps 5 GHz 16-QAM-OFDM data signal (**a**) before TPGE and (**b**) after TPGE [26].

Compared with the previous nonlinear analog equalizers, digital nonlinear equalizers are more widely studied and utilized to process received signals. The most common one is the nonlinear Volterra series-based equalizer (VE), which has great advantages against non-linear effects to further improve system performance. In recent years, some works compared the nonlinear VE with conventional linear equalizers. For instance, a nonlinear VE combined with adaptive bit-power loading discrete multi-tone (DMT) was employed in [62], and results show that the VE can bring more than 2 dB gain compared with linear equalization since the nonlinear VE is more effective against non-linear effects. Up to 16.6 Gbps data rate through 55 m tap water wireless optical transmission was achieved. The nonlinear VE has also been compared with the conventional linear feed-forward equalizer (FFE), where the nonlinear VE is shown to effectively reduce the impact of device nonlinearity [125]. Results show that a significant BER reduction (from 1×10^{-2} to 3×10^{-3}) is observed after changing linear FFE to nonlinear VE at 4.2 Gbps with 2 m transmission. In addition to conventional VE, the nonlinear Volterra series-based DFE (VDFE) can further mitigate the intrinsic static and dynamic non-linearity effects in the UOWC system. In [126], a nonlinear VDFE was demonstrated in carrierless amplitude and phase (CAP) modulation and compared with the linear DFE. However, since the LED is biased in the linear region of its transfer curve, the linear DFE and nonlinear VDFE have similar BER performance.

Moreover, the nonlinear VE combined with DMT was demonstrated in [64]. Due to effectively combating nonlinear effects, results show that VE can bring more than 3 dB gain on average compared with the system without VE. In a 15 m underwater channel, the system with a nonlinear equalizer can achieve 7.33 Gbps with BER lower than the 7% FEC threshold, which is 0.9 Gbps higher than the system without VE. Furthermore, the nonlinear second-order VE has been used in [28]. Results show that the VE can significantly reduce the influence of ISI, which achieved a better BER from 1×10^{-1} to 3.5×10^{-3} at 2.5 Gbps transmission under 60 m of tap water. In addition, nonlinear VE was also applied in [38] to compare with the direct hard-decision detection in the receiving offline DSP. Results show that the VE achieved low BER performance (2.5×10^{-3} compared with 5.91×10^{-2} of hard-decision detection) in a 100 m 500 Mbps UOWC system. Moreover, in Figure 8, when the data rate reaches 400 Mbps and 500 Mbps, severe ISI makes the system impossible to reduce the BER to achieve the FEC limit by using hard decision detection. However, the nonlinear VE can bring the BER below the FEC limit with minimum optical powers required for 400 Mbps and 500 Mbps being −26.4 dBm and −24.0 dBm, respectively.

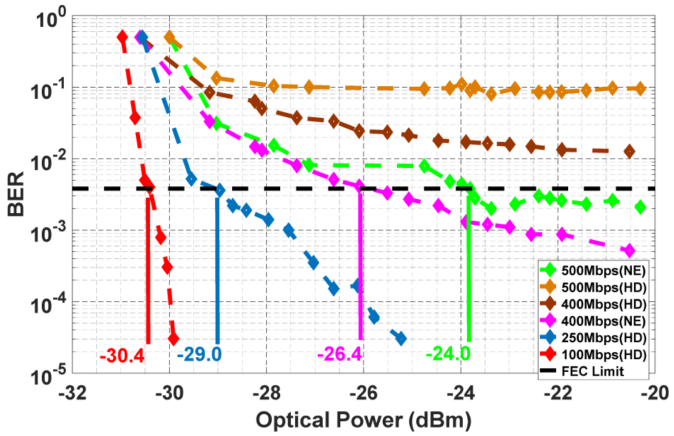

Figure 8. BER vs. received optical power for different data rates with hard-decision detection and nonlinear VE detection [38].

In addition to tap water channels, nonlinear VE has also been employed under the bubble water channel to improve the BER performance and combat ISI induced by signal light scattering from bubbles [76]. Results show that the UOWC system without the nonlinear VE can only achieve a BER below the FEC limit when the bubble size is smaller than 1.2 mm, whereas the system with VE works under bubbles with sizes up to 2.8 mm.

Compared with the conventional nonlinear VE, in which the computation complexity increases with the memory length and nonlinear order, the simpler nonlinear DFE combined with the light injection and optoelectronic feedback techniques was employed, which achieved 16 Gbps (8Gbaudps) PAM4 signal transmission in a UOWC system [27]. Moreover, the nonlinear memory polynomial model-based equalizer (MPE) has great advantages of faster convergence speed and lower error. After employing the nonlinear MPE in [30], the BER significantly increase from 1×10^{-2} to 5×10^{-5} at 160 Mbps under 100 m tap water. Moreover, due to the nonlinear MPE reducing the effect of ISI efficiently, a 200 Mbps data rate over 120 m and a 100 Mbps data rate over 139 m underwater transmission were achieved.

4. Machine Learning Applications in UOWC

4.1. Supervised Learning in UOWC Systems

Table 6 lists key studies in recent years on the application of ML algorithms in UOWC systems. Most ML algorithms are applied to the equalization at the receiver side to improve the BER performance and the transmission data rate. For instance, a novel Gaussian kernel-aided deep neural network (GK-DNN) equalizer shown in Figure 9 was employed for compensating the high nonlinear distortion of PAM8 UOWC channels in [50]. Because the GK-DNN treats the equalization problem as a classification problem, it has the advantage of performing both equalization and de-mapping at the same time. After being combined with the scalar-modified cascaded multi-modulus algorithm (S-MCMMA), the GK-DNN equalizer can perform linear equalization, nonlinear equalization, and de-mapping at the same time. Moreover, compared with the conventional DNN equalizer, the GK-DNN equalizer can reduce required training iterations by 47.06%. Results show that the BER can be significantly reduced by 1.78 dB in the LED-based UOWC system employing the GK-DNN equalizer.

Table 6. Recent research progress in the UOWC system based on supervised ML.

Year	Bit Rate (bps)	Distance	Optical Source	Receiver	Transmitter Power	Modulation Scheme	ML Algorithm	Refs.
2018	1.5 G	1.2 m Tap	457 nm LED	PIN PD	N/A	PAM8	GK-DNN	[50]
2019	N/A	1 m Turbid	532 nm LD	CCD	~20 mW	N/A	CNN	[116]
2020	3.2 G	1.2 m Tap	Blue LED	PIN PD	N/A	64-QAM	DBMLP	[111]
2020	N/A	1.2 m Tap	Blue LED	PIN PD	N/A	64-QAM	TFDNet	[112]
2021	N/A	4.3 m Turbu	632.8 nm LD	Camera	~2 mW	N/A	CNN	[117]
2021	2.85 G	1.2 m Tap	Blue LED	PIN PD	N/A	64-QAM	PCVNN	[113]
2021	N/A	30 m Coastal	Blue LED	PD	N/A	QAM	BDNet	[105]
2021	3.1 G	1.2 m Tap	Blue LED	PIN PD	~100 mW	64-QAM	TL-DBMLPs	[114]
2022	1 M	1.5 m Tap	450 nm LED	SPAD	~ 1 W	OOK	DNN	[127]
2023	660 M	90 m Tap	450 nm LD	PMT	~188.8 mW	I-SC-FDM	SWI-DNN	[115]

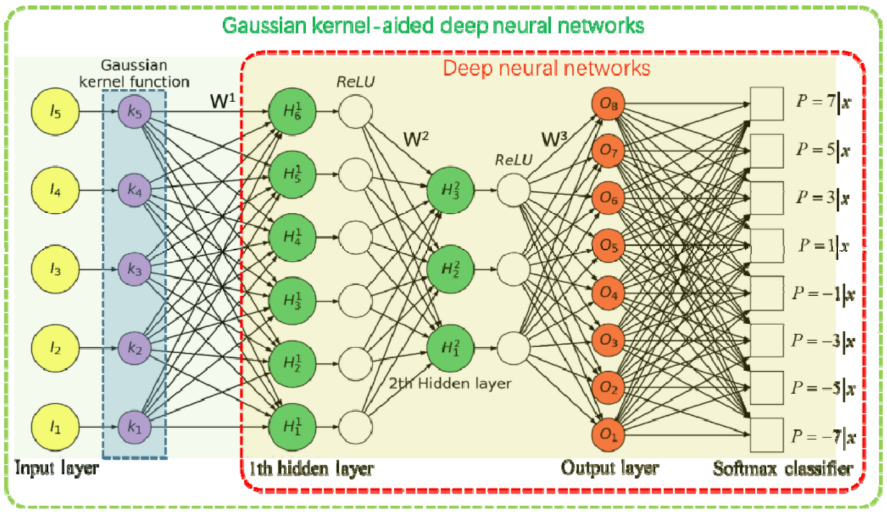

Figure 9. Structure of the GK-DNN [50].

Moreover, in [111], a dual-branch multilayer perceptron (DBMLP)-based equalizer was employed in UOWC systems. Due to the limitation on the order of the Volterra series, the nonlinear distortion in the received signal cannot be compensated accurately in conventional NML VE. Unlike NML VE, the deep neural network-based equalizer has a better capability to compensate for nonlinear distortions as it can model arbitrary mappings at arbitrary progress. Results show that the UOWC system succeeded in achieving 3.2 Gbps data transmission. Compared with the conventional VE, 63.5% BER performance enhancement and 33.8% better space complexity are achieved with the proposed DBMLP scheme. In [112,128,129], a nonlinear ML post equalizer based on the time-frequency domains deep neural network (TFDNet) was proposed in UOWC systems, as shown in Figure 10. The short-time Fourier transformation (STFT) was employed to combine the signal from two one-dimension (time domain and frequency domain) images to a two-dimension (time-frequency domain) image. Then, the signal 2D time-frequency image is fed into the DNN, which learns the mapping relations to equalize the signal to match the labeled 2D time-frequency image. Unlike the conventional DNN-based equalizers that consider only the time domain, the additional frequency domain information enables the DNN to learn complementary signal characteristics. The proposed TFDNet-based equalizers can improve the BER from 2×10^{-2} (VE) and 7×10^{-3} (DNN-based equalizer) to 2×10^{-3} at a valid operating Vpp of 0.8 V in a 2.85 Gbps UOWC system to achieve FEC limits.

Furthermore, in [113], an adaptive constellation-partitioned equalizer based on a complex-valued neural network (PCVNN) was employed to reduce the computational complexity in typical ML algorithms in UOWC systems. Experimental results show that compared with conventional ML equalizers, the computation cost can be reduced by 56.1% in the proposed PCVNN scheme in a 2.85 Gbps UOWC system. Two transfer learning-based (TL) DBMLPs were demonstrated in [114]. Unlike the conventional DBMLPs, the TL-DBMLP is more robust to the jitter of LED transmitter bias current and also requires a

smaller number of training epochs. Experimental results show that the proposed UOWC system employing TL-DBMLPs can reduce the size of the training set from 50% to 10% of the total dataset to achieve an acceptable mean square error (MSE). Moreover, with only 10 epochs, the achievable BER is improved from 1×10^{-2} with conventional DBMLPs to 1×10^{-3} using the TL-DBMLPs. Moreover, a novel sparse weight-initiated deep neural network (SWI-DNN) equalizer combined with the interleaved single-carrier frequency division multiplexing (I-SC-FDM) scheme was employed for UOWC systems in [115]. Due to the implementation of a special SWI structure, the necessary training epochs of the SWI-DNN equalizer can be reduced by 10.3%. Results show that to achieve the BER of 3.8×10^{-3} (i.e., FEC limit) in the 90 m UOWC system, the data rate can be increased by 17.9% after employing the ML equalizer than conventional TFD equalizers.

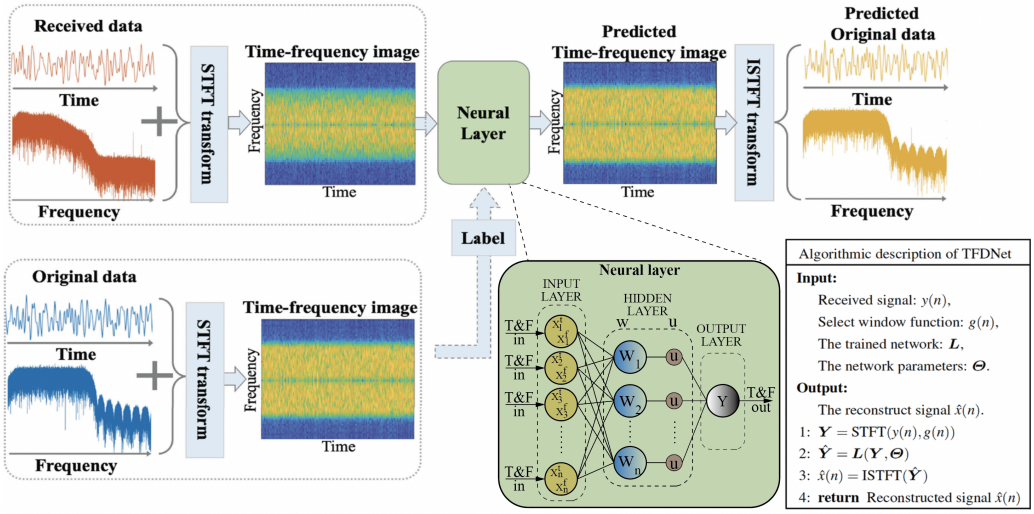

Figure 10. Schematic diagram of the proposed TFDNet [112,128].

In addition, a 16-ary orbital angular momentum shift keying (OAM-SK) equalizer based on convolutional neural networks (CNNs) was proposed in [116]. Results show that ML schemes can achieve an accuracy of more than 96% and a larger number of pixels in the camera receiver can be utilized in a camera-based UOWC system. Hence, the ML-based equalizer can significantly improve the accuracy of data decoding. In addition, the other equalizer based on CNNs was employed in [117]. They succeed in achieving a high accuracy (93.7∼99.9%) in high-turbulence UOWC with a camera-based receiver for image transmission. A larger alphabet and faster classification rates can be achieved in LD-based UOWC systems. In [105], a new equalizer based on a blind detection network (BDNet) was considered in UOWC systems. Unlike the previous blind channel estimation (BCE) schemes, the BDNet has the advantage of estimating the inverse channel regardless of the scalar ambiguity issue by learning the latent channel features from the received signal only. Simulation results show that the proposed UOWC with the BDNet achieves better BER performance compared with conventional BCE schemes. In addition, ML algorithms have also been studied for time synchronization and clock recovery in UOWC systems. The recovery of the time slot synchronous in the photon-counting UOWC system is critical, and conventionally it is realized based on symbol synchronization and frame synchronization, which has limited accuracy. To predict the phase value of the time slot synchronous clock, a method of time slot synchronous clock recovery for photon-counting UOWC based on DNNs is designed in [127]. Results show that the photon-counting UOWC based on the ML time slot synchronous clock recovery succeeded in achieving a data rate of 1 Mbps and a BER of 5.35×10^{-4} at eight photons per time slot.

4.2. Reinforcement Learning in UOWC Systems

Reinforcement learning is often used in UOWC systems to improve the connection success rate of the underwater sensor network and AUVs, further increasing the reliability of links. In underwater sensor networks, the highly dynamic topology can hinder the routing of UOWC links, particularly due to the ocean flow movement. In [121], an advanced routing protocol based on multi-agent reinforcement learning (MARL) was proposed to increase the link reliability and communication quality in the UOWC-based sensor network. Simulation results show that the UOWC-based sensor network with MARL has 80% average residual energy of the network after 150 simulation times compared with 30% and 70% achieved with the Q-learning-based delay tolerant routing (QDTR) and the ad hoc on-demand distance vector (AODV) routing protocols. Moreover, MARL has the highest delivery ratio in the static network (95.87%) and the dynamic network (95.57%) compared with the other two schemes (49.5% and 44.56% achieved in AODV in the static network and the dynamic network, respectively). In addition, to overcome the same limitations, an efficient routing protocol based on MARL was also employed in another work [122]. Simulation results show that the MARL routing protocol provided the same low power consumption advantages and high-quality UOWC linksin a network with 14 neighboring nodes.

Moreover, reinforcement learning algorithms have also been exploited to solve pointing acquisition and tracking (PAT) problems between underwater applications (AUVs). An advanced beam adaptation method based on the state–action–reward–state–action (SARSA) algorithm for point-to-point UOWC systems was proposed in [118]. Results show that the SARSA-based beam adaptation method increased the success rate from 66% to 93%, which further achieved better link reliability. Moreover, the SARSA increased SNR by 6 to 10 dB compared to the traditional NML method in different types of underwater channels. Similarly, to overcome the poor link reliability and to optimize the connecting success rates between two AUVs, the soft actor-critic reinforcement learning algorithm was designed in [119]. Results show that the success rate for the transmitting AUV to maintain the LOS link for ten time steps was 97.53% after 10,000 episodes in the simulation environment. In [120], a deep reinforcement learning algorithm assisted by an extended Kalman filter was employed to improve the reliability of water–air optical wireless communication between AUVs and unmanned aerial vehicles (UAVs), which is even more challenging compared with connecting AUVs only. Results show that the proposed learning algorithm achieves a shorter MSE (0.02 m) compared with the triangular exploration (TE) algorithm (0.06 m), a shorter flight distance (1.1 m compared to 2 m on TE), and a smoother trajectory (3.23 compared to 6.98 on TE), which implies a higher alignment accuracy and smaller energy consumption. Moreover, it also improves the link availability by 25% compared with the TE algorithm.

5. Discussion and Future Scope

Although a promising solution, UOWC systems face the key challenge of ISI caused by signal scattering in underwater channels. To improve the data transmission distance and improve the BER, various types of equalizers have been proposed and studied, as discussed in detail in Section 3. Both linear and nonlinear equalizers have been investigated, and better BER and higher data rates in UOWC systems have been achieved. However, linear equalizers have the limitations of only being capable of stable communication channels. When the channel is disturbed, the performance of the linear equalizer is degraded significantly. In addition, they cannot suppress the nonlinear effects that widely exist in UOWC systems. On the other hand, nonlinear equalizers can suppress various types of nonlinearities in UOWC systems, and hence, have enhanced capability to improve data transmission performance. However, they normally have complex equalizer structures. Although the nonlinear equalizer configurations can be adjusted according to the influence of non-linearity, the variable underwater channel environment limits equalizer adjustment efficiency.

With the advancement of artificial intelligence, ML equalizers have been studied as well and have shown unique advantages over traditional NML equalizers. They can learn from the received signal to equalize signals in different underwater channels, noises, and system geometric arrangements. In particular, ML equalizers have enhanced capability in suppressing nonlinear effects in UOWC systems. ML equalizers can also handle multiple impairments simultaneously, effectively solving the interactions among different impairments. However, ML equalizers also face a number of key challenges. More complicated algorithms are typically required in complex environments, and these algorithms require a large number of training datasets and iterations, which often take a long time and are computationally expensive, requiring high-end hardware. Some recent research [113–115] starts to optimize the algorithms and reduce the training epochs to reduce the memory and time cost of ML equalizers. Solving this challenge becomes one focus of future UOWC post-signal processing technology.

Future underwater communication applications will certainly rely on reliable and powerful signal processing techniques to improve the system BER and performance. Adaptive equalizations can be a promising future research direction. For instance, in a calm lake or clear ocean, which has a stable underwater channel with limited nonlinear effect, a low-cost and simple linear equalizer can operate efficiently. In windy and choppy seas, nonlinear equalizers can be employed to reduce nonlinear effects and improve system performance. Finally, in challenging underwater channels such as turbidity and harbor water, variable impurities and underwater turbulence cause substantial changes in signal transmission. Traditional NML equalizers have limited capability in such complex and variable underwater channels. Instead, ML equalizers can automatically learn according to different channel performances and system configurations to optimize the performance of equalizing signals. However, since complex algorithms lead to a long training time and a larger number of training iterations, developing efficient hardware accelerators in ML-based equalizers can also be a future research field. Furthermore, so far the signal processing is mostly considered in point-to-point direct links. With the relay concept being considered in UOWC networks, the corresponding signal processing technique can be another research direction.

6. Conclusions

In this article, we provided a structured review of recent progress in UOWC systems, which are in high demand to overcome the inherent limitations of conventional acoustic systems and provide high-speed wireless communication links in underwater environments. In particular, we focused on the signal processing aspect of UOWC systems, which has attracted intensive interest as a promising method to suppress signal generation, modulation, transmission, and reception impairments. We reviewed the recent progress on both ML- and NML-based signal processing techniques. Due to its simple structure, the traditional NML equalization techniques can efficiently solve the SNR reduction caused by ISI, thereby improving the data rate of UOWC systems in recent years. Due to the advancement and development of ML algorithms, ML-based equalization techniques have shown better capability in reducing the influence of nonlinear effects. However, ML-based schemes normally require complex algorithms and powerful hardware support (high-performance computers).

In practical applications, water flow, temperature, and sunlight are changing all the time. Hence, considering the dynamic feature of underwater channels, designing adaptive signal processing techniques is important in the future, which is a key challenge in current studies. In addition, whereas the ML algorithm can achieve impressive results by suppressing both linear and nonlinear impairments effectively, the training process is complicated, requires a large number of computations, and takes a long time. Some recent ML research has begun to optimize algorithms to reduce the training epochs of ML-based equalizers to improve DSP efficiency and reduce computation costs. With the continuous development of hardware and continuous innovation of algorithms, the computation-efficient ML algo-

rithms for UOWC systems will be a key research focus in the future. Moreover, due to the dynamic topology problem caused by water flow, the underwater sensor network needs a more intelligent way to ensure stable links. According to recent research, the UOWC network based on reinforcement learning can greatly improve communication success rate and stability, providing a promising solution for future UOWC applications.

Author Contributions: Conceptualization, C.F. and K.W.; software, Y.W.; writing—original draft preparation, C.F.; writing—review and editing, C.F., S.L., Y.W. and K.W.; visualization, Y.W.; supervision, S.L. and K.W. All authors have read and agreed to the published version of the manuscript.

Funding: This research was funded by the Australian Research Council (ARC) under Grant DP170100268.

Institutional Review Board Statement: Not applicable.

Informed Consent Statement: Not applicable.

Data Availability Statement: Not applicable.

Conflicts of Interest: The authors declare no conflict of interest.

Abbreviations

The following abbreviations are used in this manuscript:

Air	Air Free Space Channel
AMP	Amplifier
AODV	Ad Hoc on-Demand Distance Vector
APD	Avalanche Photodiode
APE	Analog Post-Equalizer
AUV	Autonomous Underwater Vehicle
BCE	Blind Channel Estimation
BDNet	Blind Detection Network
BER	Bit-Error-Rate
Bubble	Bubble Water Channel
CAP	Carrierless Amplitude and Phase
CCD	Charge-Coupled Device
Clear	Clear Ocean Channel
CNN	Convolutional Neural Network
Coastal	Coastal Water Channel
DAC	Digital-to-Analog Converter
DBMLP	Dual-Branch Multilayer Perceptron
DFE	Decision-Feedback Equalizer
DMT	Discrete Multi-Tone
DNN	Deep Neural Network
DSP	Digital Signal Processing
FDE	Frequency Domain Equalizer
FEC	Forward Error Correction
FFE	Feedforward Equalizer
FSO	Free-Space Optical
GaN	Gallium Nitride
GK	Gaussian Kernel-aided
Harbor	Harbor Water Channel
HG	Henyey–Greenstein
IoUT	Internet of Underwater Things
I-SC-FDM	Interleaved Single-Carrier Frequency Division Multiplexing
ISI	Inter-Symbol Interference
LD	Laser Diode
LE	Linear Equalizers

LED	Light-Emitting Diode
LOS	Line-of-Sight
MAC	Medium Access Control
MARL	Multi-agent Reinforcement Learning
MC	Monte Carlo
MIMO	Multiple-Input Multiple-Output
ML	Machine Learning
MMSE	Minimum Mean Square Error
MPE	Memory Polynomial Model-Based Equalizer
MSE	Mean-Square Error
NLE	Nonlinear Equalizers
NLOS	Non-Line-of-Sight
NML	Non-Machine Learning
NP	Noise Prediction
NRZ	No Return to Zero
OAM-SK	Orbital Angular Momentum Shift Keying
OBS	Optical Base Station
OFDM	Orthogonal Frequency-Division Multiplexing
OOK	On–Off Keying
PAM	Pulse Amplitude Modulation
PAT	Pointing Acquisition and Tracking
PCVNN	Partitioned Equalizer Based on Complex-Valued Neural Network
PD	Photodiode
PIN PD	PIN Photodiode
PMT	Photo-Multiplier Tube
PPM	Pulse Position Modulation
QAM	Quadrature Amplitude Modulation
QDTR	Q-Learning-Based Delay Tolerant Routing
RF	Radio Frequency
RRC	Root Raised Cosine
SARSA	State–Action–Reward–State–Action
SiPM	Silicon Photo-Multipliers
SNR	Signal-to-Noise Ratio
SPAD	Single-Photon Avalanche Diode
SPF	Scattering Phase Function
STFT	Short Time Fourier Transformation
SWI	Sparse Weight-Initiated
Tap	Tap Water Channel
TE	Triangular Exploration
TFDNet	Time-Frequency Domains Deep Neural Network
TL	Two Transfer Learning
TPGE	Tunable Passive Gain Equalizer
TTHG	Two-term Henyey–Greenstein
Turbu	Turbulence Water Channel
Turbid	Turbid Water Channel
UAC	Underwater Acoustic Communication
UAV	Unmanned Aerial Vehicle
UM	Underwater Monitor
UOT	Underwater Optical Turbulence
UOWC	Underwater Optical Wireless Communication
UWC	Underwater Wireless Communication
VDFE	Volterra Series-Based Decision-Feedback Equalizer
VE	Volterra Series-Based Equalizer
ZF	Zero-Forcing

References

1. Woodruff, S.D.; Slutz, R.J.; Jenne, R.L.; Steurer, P.M. A comprehensive ocean-atmosphere data set. *Bull. Am. Meteorol. Soc.* **1987**, *68*, 1239–1250. [CrossRef]
2. Saeed, N.; Celik, A.; Al-Naffouri, T.Y.; Alouini, M.S. Underwater optical wireless communications, networking, and localization: A survey. *Ad Hoc Netw.* **2019**, *94*, 101935. [CrossRef]
3. Hoeher, P.A.; Sticklus, J.; Harlakin, A. Underwater optical wireless communications in swarm robotics: A tutorial. *IEEE Commun. Surv. Tutor.* **2021**, *23*, 2630–2659. [CrossRef]
4. Sozer, E.; Stojanovic, M.; Proakis, J. Underwater acoustic networks. *IEEE J. Ocean. Eng.* **2000**, *25*, 72–83. [CrossRef]
5. Kida, Y.; Deguchi, M.; Shimura, T. Experimental result for a high-rate underwater acoustic communication in deep sea for a manned submersible shinkai6500. *J. Mar. Acoust. Soc. Jpn.* **2018**, *45*, 197–203. [CrossRef]
6. Song, H.; Hodgkiss, W. Efficient use of bandwidth for underwater acoustic communication. *J. Acoust. Soc. Am.* **2013**, *134*, 905–908. [CrossRef]
7. Akyildiz, I.F.; Pompili, D.; Melodia, T. Challenges for efficient communication in underwater acoustic sensor networks. *ACM Sigbed Rev.* **2004**, *1*, 3–8. [CrossRef]
8. Kaushal, H.; Kaddoum, G. Underwater optical wireless communication. *IEEE Access* **2016**, *4*, 1518–1547. [CrossRef]
9. Al-Shamma'a, A.I.; Shaw, A.; Saman, S. Propagation of electromagnetic waves at MHz frequencies through seawater. *IEEE Trans. Antennas Propag.* **2004**, *52*, 2843–2849. [CrossRef]
10. Tian, P.; Liu, X.; Yi, S.; Huang, Y.; Zhang, S.; Zhou, X.; Hu, L.; Zheng, L.; Liu, R. High-speed underwater optical wireless communication using a blue GaN-based micro-LED. *Opt. Express* **2017**, *25*, 1193–1201. [CrossRef]
11. Lee, C.; Zhang, C.; Cantore, M.; Farrell, R.M.; Oh, S.H.; Margalith, T.; Speck, J.S.; Nakamura, S.; Bowers, J.E.; DenBaars, S.P. 4 Gbps direct modulation of 450 nm GaN laser for high-speed visible light communication. *Opt. Express* **2015**, *23*, 16232–16237. [CrossRef]
12. Alghamdi, R.; Saeed, N.; Dahrouj, H.; Alouini, M.S.; Al-Naffouri, T.Y. Towards ultra-reliable low-latency underwater optical wireless communications. In Proceedings of the 2019 IEEE 90th Vehicular Technology Conference (VTC2019-Fall), IEEE, Honolulu, HI, USA, 22–25 September 2019; pp. 1–6.
13. Zhu, S.; Chen, X.; Liu, X.; Zhang, G.; Tian, P. Recent progress in and perspectives of underwater wireless optical communication. *Prog. Quantum Electron.* **2020**, *73*, 100274. [CrossRef]
14. Chen, H.; Chen, X.; Lu, J.; Liu, X.; Shi, J.; Zheng, L.; Liu, R.; Zhou, X.; Tian, P. Toward long-distance underwater wireless optical communication based on a high-sensitivity single photon avalanche diode. *IEEE Photonics J.* **2020**, *12*, 1–10. [CrossRef]
15. Zeng, Z.; Fu, S.; Zhang, H.; Dong, Y.; Cheng, J. A survey of underwater optical wireless communications. *IEEE Commun. Surv. Tutor.* **2016**, *19*, 204–238. [CrossRef]
16. Murgod, T.R.; Sundaram, S.M. Survey on underwater optical wireless communication: Perspectives and challenges. *Indones. J. Electr. Eng. Comput. Sci.* **2019**, *13*, 138–146. [CrossRef]
17. Schirripa Spagnolo, G.; Cozzella, L.; Leccese, F. Underwater optical wireless communications: Overview. *Sensors* **2020**, *20*, 2261. [CrossRef] [PubMed]
18. Mohsan, S.A.H.; Hasan, M.M.; Mazinani, A.; Sadiq, M.A.; Akhtar, M.H.; Islam, A.; Rokia, L.S. A systematic review on practical considerations, recent advances and research challenges in underwater optical wireless communication. *Int. J. Adv. Comput. Sci. Appl.* **2020**, *11*. [CrossRef]
19. Oubei, H.M.; Shen, C.; Kammoun, A.; Zedini, E.; Park, K.H.; Sun, X.; Liu, G.; Kang, C.H.; Ng, T.K.; Alouini, M.S.; et al. Light based underwater wireless communications. *Jpn. J. Appl. Phys.* **2018**, *57*, 08PA06. [CrossRef]
20. Geldard, C.T.; Thompson, J.; Popoola, W.O. An overview of underwater optical wireless channel modelling techniques. In Proceedings of the 2019 International Symposium on Electronics and Smart Devices (ISESD), IEEE, Badung, Indonesia, 8–9 October 2019; pp. 1–4.
21. Miroshnikova, N.; Petruchin, G.; Sherbakov, A. Problems of underwater optical links modeling. In Proceedings of the 2019 Systems of Signal Synchronization, Generating and Processing in Telecommunications (SYNCHROINFO), IEEE, Russia, 1–3 July 2019; pp. 1–9.
22. Liu, W.; Xu, Z.; Yang, L. SIMO detection schemes for underwater optical wireless communication under turbulence. *Photonics Res.* **2015**, *3*, 48–53. [CrossRef]
23. Baykal, Y.; Ata, Y.; Gökçe, M.C. Underwater turbulence, its effects on optical wireless communication and imaging: A review. *Opt. Laser Technol.* **2022**, *156*, 108624. [CrossRef]
24. Nguyen, C.T.; Nguyen, M.T.; Mai, V.V. Underwater optical wireless communication-based IoUT networks: MAC performance analysis and improvement. *Opt. Switch. Netw.* **2020**, *37*, 100570. [CrossRef]
25. Li, X.; Cheng, C.; Zhang, C.; Wei, Z.; Wang, L.; Fu, H.; Yang, Y. Net 4 Gb/s underwater optical wireless communication system over 2 m using a single-pixel GaN-based blue mini-LED and linear equalization. *Opt. Lett.* **2022**, *47*, 1976–1979. [CrossRef]
26. Lu, H.H.; Li, C.Y.; Lin, H.H.; Tsai, W.S.; Chu, C.A.; Chen, B.R.; Wu, C.J. An 8 m/9.6 Gbps underwater wireless optical communication system. *IEEE Photonics J.* **2016**, *8*, 1–7. [CrossRef]
27. Li, C.Y.; Lu, H.H.; Tsai, W.S.; Cheng, M.T.; Ho, C.M.; Wang, Y.C.; Yang, Z.Y.; Chen, D.Y. 16 Gb/s PAM4 UWOC system based on 488-nm LD with light injection and optoelectronic feedback techniques. *Opt. Express* **2017**, *25*, 11598–11605. [CrossRef]

28. Lu, C.; Wang, J.; Li, S.; Xu, Z. 60 m/2.5 Gbps underwater optical wireless communication with NRZ-OOK modulation and digital nonlinear equalization. In Proceedings of the 2019 Conference on Lasers and Electro-Optics (CLEO), IEEE, San Jose, CA, USA, 5–10 May 2019; pp. 1–2.
29. Liu, A.; Zhang, R.; Lin, B.; Yin, H. Multi-degree-of-freedom for underwater optical wireless communication with improved transmission performance. *J. Mar. Sci. Eng.* **2022**, *11*, 48. [CrossRef]
30. Yang, X.; Tong, Z.; Dai, Y.; Chen, X.; Zhang, H.; Zou, H.; Xu, J. 100 m full-duplex underwater wireless optical communication based on blue and green lasers and high sensitivity detectors. *Opt. Commun.* **2021**, *498*, 127261. [CrossRef]
31. Alkhasraji, J.; Tsimenidis, C. Coded OFDM over short range underwater optical wireless channels using LED. In Proceedings of the Oceans 2017-Aberdeen, IEEE, Aberdeen, UK, 19–22 June 2017; pp. 1–7.
32. Chauhan, D.S.; Kaur, G.; Kumar, D. Design of novel MIMO UOWC link using gamma—Gamma fading channel for IoUTs. *Opt. Quantum Electron.* **2022**, *54*, 512. [CrossRef]
33. Bai, J.; Li, N.; Nie, J.; Liang, X. Power Optimization of UOWC-MIMO-OFDM System Based on PSO-WF Algorithm. *J. Phys. Conf. Ser.* **2023**, *2476*, 012075. [CrossRef]
34. Huang, A.; Tao, L.; Jiang, Q. BER performance of underwater optical wireless MIMO communications with spatial modulation under weak turbulence. In Proceedings of the 2018 OCEANS-MTS/IEEE Kobe Techno-Oceans (OTO), IEEE, Kobe, Japan, 28–31 May 2018; pp. 1–5.
35. Tsai, W.S.; Lu, H.H.; Wu, H.W.; Su, C.W.; Huang, Y.C. A 30 Gb/s PAM4 underwater wireless laser transmission system with optical beam reducer/expander. *Sci. Rep.* **2019**, *9*, 8605. [CrossRef]
36. Tu, C.; Liu, W.; Jiang, W.; Xu, Z. First Demonstration of 1 Gb/s PAM4 Signal Transmission Over A 130 m Underwater Optical Wireless Communication Channel with Digital Equalization. In Proceedings of the 2021 IEEE/CIC International Conference on Communications in China (ICCC), IEEE, Xiamen, China, 28–30 July 2021; pp. 853–857.
37. Tang, S.; Dong, Y.; Zhang, X. Impulse response modeling for underwater wireless optical communication links. *IEEE Trans. Commun.* **2013**, *62*, 226–234. [CrossRef]
38. Wang, J.; Lu, C.; Li, S.; Xu, Z. 100 m/500 Mbps underwater optical wireless communication using an NRZ-OOK modulated 520 nm laser diode. *Optics Express* **2019**, *27*, 12171–12181. [CrossRef] [PubMed]
39. Hanson, F.; Radic, S. High bandwidth underwater optical communication. *Appl. Opt.* **2008**, *47*, 277–283. [CrossRef] [PubMed]
40. Oubei, H.M.; Li, C.; Park, K.H.; Ng, T.K.; Alouini, M.S.; Ooi, B.S. 2.3 Gbit/s underwater wireless optical communications using directly modulated 520 nm laser diode. *Opt. Express* **2015**, *23*, 20743–20748. [CrossRef] [PubMed]
41. Wang, P.; Li, C.; Xu, Z. A cost-efficient real-time 25 Mb/s system for LED-UOWC: Design, channel coding, FPGA implementation, and characterization. *J. Light. Technol.* **2018**, *36*, 2627–2637. [CrossRef]
42. Tsai, C.L.; Lu, Y.C.; Chang, S.H. InGaN LEDs fabricated with parallel-connected multi-pixel geometry for underwater optical communications. *Opt. Laser Technol.* **2019**, *118*, 69–74. [CrossRef]
43. Han, B.; Zhao, W.; Zheng, Y.; Meng, J.; Wang, T.; Han, Y.; Wang, W.; Su, Y.; Duan, T.; Xie, X. Experimental demonstration of quasi-omni-directional transmitter for underwater wireless optical communication based on blue LED array and freeform lens. *Opt. Commun.* **2019**, *434*, 184–190. [CrossRef]
44. Hu, S.; Mi, L.; Zhou, T.; Chen, W. 35.88 attenuation lengths and 3.32 bits/photon underwater optical wireless communication based on photon-counting receiver with 256-PPM. *Opt. Express* **2018**, *26*, 21685–21699. [CrossRef]
45. Shen, J.; Wang, J.; Yu, C.; Chen, X.; Wu, J.; Zhao, M.; Qu, F.; Xu, Z.; Han, J.; Xu, J. Single LED-based 46-m underwater wireless optical communication enabled by a multi-pixel photon counter with digital output. *Opt. Commun.* **2019**, *438*, 78–82. [CrossRef]
46. Cochenour, B.; Mullen, L.; Muth, J. A modulated pulse laser for underwater detection, ranging, imaging, and communications. In Proceedings of the Ocean Sensing and Monitoring IV. SPIE, Baltimore, MD, USA, 23–27 April 2012; Volume 8372, pp. 217–226.
47. Wang, Z.; Dong, Y.; Zhang, X.; Tang, S. Adaptive modulation schemes for underwater wireless optical communication systems. In Proceedings of the 7th International Conference on Underwater Networks & Systems, Los Angeles, CA, USA, 5–6 November 2012; pp. 1–2.
48. Kong, M.; Chen, Y.; Sarwar, R.; Sun, B.; Xu, Z.; Han, J.; Chen, J.; Qin, H.; Xu, J. Underwater wireless optical communication using an arrayed transmitter/receiver and optical superimposition-based PAM-4 signal. *Opt. Express* **2018**, *26*, 3087–3097. [CrossRef]
49. Zhuang, B.; Li, C.; Wu, N.; Xu, Z. First demonstration of 400 Mb/s PAM4 signal transmission over 10-meter underwater channel using a blue LED and a digital linear pre-equalizer. In Proceedings of the 2017 Conference on Lasers and Electro-Optics (CLEO), IEEE, San Jose, CA, USA, 14–19 May 2017; pp. 1–2.
50. Chi, N.; Zhao, Y.; Shi, M.; Zou, P.; Lu, X. Gaussian kernel-aided deep neural network equalizer utilized in underwater PAM8 visible light communication system. *Opt. Express* **2018**, *26*, 26700–26712. [CrossRef]
51. Wang, J.; Yang, X.; Lv, W.; Yu, C.; Wu, J.; Zhao, M.; Qu, F.; Xu, Z.; Han, J.; Xu, J. Underwater wireless optical communication based on multi-pixel photon counter and OFDM modulation. *Opt. Commun.* **2019**, *451*, 181–185. [CrossRef]
52. Huang, X.H.; Li, C.Y.; Lu, H.H.; Su, C.W.; Wu, Y.R.; Wang, Z.H.; Chen, Y.N. 6-m/10-Gbps underwater wireless red-light laser transmission system. *Opt. Eng.* **2018**, *57*, 066110. [CrossRef]
53. Wu, T.C.; Chi, Y.C.; Wang, H.Y.; Tsai, C.T.; Lin, G.R. Blue laser diode enables underwater communication at 12.4 Gbps. *Sci. Rep.* **2017**, *7*, 40480. [CrossRef] [PubMed]
54. Wang, F.; Liu, Y.; Shi, M.; Chen, H.; Chi, N. 3.075 Gb/s underwater visible light communication utilizing hardware pre-equalizer with multiple feature points. *Opt. Eng.* **2019**, *58*, 056117. [CrossRef]

55. Li, J.; Wang, F.; Zhao, M.; Jiang, F.; Chi, N. Large-coverage underwater visible light communication system based on blue LED employing equal gain combining with integrated PIN array reception. *Appl. Opt.* **2019**, *58*, 383–388. [CrossRef]
56. Wang, F.; Liu, Y.; Jiang, F.; Chi, N. High speed underwater visible light communication system based on LED employing maximum ratio combination with multi-PIN reception. *Opt. Commun.* **2018**, *425*, 106–112. [CrossRef]
57. Zhang, Z.; Lai, Y.; Lv, J.; Liu, P.; Teng, D.; Wang, G.; Liu, L. Over 700 MHz–3 dB bandwidth UOWC system based on blue HV-LED with T-bridge pre-equalizer. *IEEE Photonics J.* **2019**, *11*, 1–12. [CrossRef]
58. Arvanitakis, G.N.; Bian, R.; McKendry, J.J.; Cheng, C.; Xie, E.; He, X.; Yang, G.; Islim, M.S.; Purwita, A.A.; Gu, E.; et al. Gb/s underwater wireless optical communications using series-connected GaN micro-LED arrays. *IEEE Photonics J.* **2019**, *12*, 1–10. [CrossRef]
59. Hong, X.; Fei, C.; Zhang, G.; Du, J.; He, S. Discrete multitone transmission for underwater optical wireless communication system using probabilistic constellation shaping to approach channel capacity limit. *Opt. Lett.* **2019**, *44*, 558–561. [CrossRef]
60. Li, C.Y.; Lu, H.H.; Tsai, W.S.; Wang, Z.H.; Hung, C.W.; Su, C.W.; Lu, Y.F. A 5 m/25 Gbps underwater wireless optical communication system. *IEEE Photonics J.* **2018**, *10*, 1–9. [CrossRef]
61. Oubei, H.M.; Duran, J.R.; Janjua, B.; Wang, H.Y.; Tsai, C.T.; Chi, Y.C.; Ng, T.K.; Kuo, H.C.; He, J.H.; Alouini, M.S.; et al. 4.8 Gbit/s 16-QAM-OFDM transmission based on compact 450-nm laser for underwater wireless optical communication. *Opt. Express* **2015**, *23*, 23302–23309. [CrossRef]
62. Fei, C.; Hong, X.; Zhang, G.; Du, J.; Gong, Y.; Evans, J.; He, S. 16.6 Gbps data rate for underwater wireless optical transmission with single laser diode achieved with discrete multi-tone and post nonlinear equalization. *Opt. Express* **2018**, *26*, 34060–34069. [CrossRef]
63. Chen, X.; Lyu, W.; Zhang, Z.; Zhao, J.; Xu, J. 56-m/3.31-Gbps underwater wireless optical communication employing Nyquist single carrier frequency domain equalization with noise prediction. *Opt. Express* **2020**, *28*, 23784–23795. [CrossRef]
64. Fei, C.; Zhang, J.; Zhang, G.; Wu, Y.; Hong, X.; He, S. Demonstration of 15-M 7.33-Gb/s 450-nm underwater wireless optical discrete multitone transmission using post nonlinear equalization. *J. Light. Technol.* **2018**, *36*, 728–734. [CrossRef]
65. Pandey, P.; Agrawal, M. High speed and Long range underwater optical wireless communication. In Proceedings of the Global Oceans 2020: Singapore–US Gulf Coast, IEEE, Biloxi, MS, USA, 5–30 October 2020; pp. 1–10.
66. Kaeib, F.; Alshawish, O.A.; Altayf, S.A.; Gamoudi, M.A. Designing and Analysis of Underwater Optical Wireless communication system. In Proceedings of the 2022 IEEE 2nd International Maghreb Meeting of the Conference on Sciences and Techniques of Automatic Control and Computer Engineering (MI-STA), IEEE, Sabratha, Libya, 23–25 May 2022; pp. 441–446.
67. Pandey, P.; Matta, G.; Aggarwal, M. Performance comparisons between Avalanche and PIN photodetectors for use in underwater optical wireless communication systems. In Proceedings of the OCEANS 2021: San Diego–Porto, IEEE, San Diego, CA, USA, 20–23 September 2021; pp. 1–8.
68. Mobley, C. *Light and Water: Radiative Transfer in Natural Water*; Academic Press: San Diego, CA, USA, 1994.
69. Mobley, C.D.; Gentili, B.; Gordon, H.R.; Jin, Z.; Kattawar, G.W.; Morel, A.; Reinersman, P.; Stamnes, K.; Stavn, R.H. Comparison of numerical models for computing underwater light fields. *Appl. Opt.* **1993**, *32*, 7484–7504. [CrossRef]
70. Duntley, S.Q. Light in the sea. *JOSA* **1963**, *53*, 214–233. [CrossRef]
71. Haltrin, V.I. Chlorophyll-based model of seawater optical properties. *Appl. Opt. (2004)* **1999**, *38*, 6826–6832. [CrossRef] [PubMed]
72. Shen, C.; Guo, Y.; Oubei, H.M.; Ng, T.K.; Liu, G.; Park, K.H.; Ho, K.T.; Alouini, M.S.; Ooi, B.S. 20-meter underwater wireless optical communication link with 1.5 Gbps data rate. *Opt. Express* **2016**, *24*, 25502–25509. [CrossRef]
73. Johnson, L.J.; Green, R.J.; Leeson, M.S. Underwater optical wireless communications: Depth dependent variations in attenuation. *Appl. Opt.* **2013**, *52*, 7867–7873. [CrossRef]
74. Yap, Y.; Jasman, F.; Marcus, T. Impact of chlorophyll concentration on underwater optical wireless communications. In Proceedings of the 2018 7th International Conference on Computer and Communication Engineering (ICCCE), IEEE, Kuala Lumpur, Malaysia, 19–20 September 2018; pp. 1–6.
75. Liu, W.; Zou, D.; Xu, Z.; Yu, J. Non-line-of-sight scattering channel modeling for underwater optical wireless communication. In Proceedings of the 2015 IEEE International Conference on Cyber Technology in Automation, Control, and Intelligent Systems (CYBER), IEEE, Shenyang, China, 8–12 June 2015; pp. 1265–1268.
76. Chen, D.; Wang, J.; Li, S.; Xu, Z. Effects of air bubbles on underwater optical wireless communication. *Chin. Opt. Lett.* **2019**, *17*, 100008. [CrossRef]
77. Shin, M.; Park, K.H.; Alouini, M.S. Statistical modeling of the impact of underwater bubbles on an optical wireless channel. *IEEE Open J. Commun. Soc.* **2020**, *1*, 808–818. [CrossRef]
78. Oubei, H.M.; ElAfandy, R.T.; Park, K.H.; Ng, T.K.; Alouini, M.S.; Ooi, B.S. Performance evaluation of underwater wireless optical communications links in the presence of different air bubble populations. *IEEE Photonics J.* **2017**, *9*, 1–9. [CrossRef]
79. Tsai, W.S.; Li, C.Y.; Lu, H.H.; Lu, Y.F.; Tu, S.C.; Huang, Y.C. 256 Gb/s four-channel SDM-based PAM4 FSO-UWOC convergent system. *IEEE Photonics J.* **2019**, *11*, 1–8. [CrossRef]
80. Fang, C.; Li, S.; Wang, K. Accurate Underwater Optical Wireless Communication Model With Both Line-of-Sight and Non-Line-of-Sight Channels. *IEEE Photonics J.* **2022**, *14*, 1–12. [CrossRef]
81. Mahapatra, S.K.; Varshney, S.K. Performance of the Reed-Solomon-coded underwater optical wireless communication system with orientation-based solar light noise. *JOSA A* **2022**, *39*, 1236–1245. [CrossRef]

82. Fang, C.; Li, S.; Wang, K. Accurate underwater optical wireless communication (UOWC) channel model. In Proceedings of the Asia Communications and Photonics Conference. Optical Society of America, Shanghai, China, 24–27 October 2021; pp. T4A–143.
83. Huang, Y.F.; Tsai, C.T.; Chi, Y.C.; Huang, D.W.; Lin, G.R. Filtered multicarrier OFDM encoding on blue laser diode for 14.8-Gbps seawater transmission. *J. Light. Technol.* **2017**, *36*, 1739–1745. [CrossRef]
84. Hu, F.; Li, G.; Zou, P.; Hu, J.; Chen, S.; Liu, Q.; Zhang, J.; Jiang, F.; Wang, S.; Chi, N. 20.09-Gbit/s underwater WDM-VLC transmission based on a single Si/GaAs-substrate multichromatic LED array chip. In Proceedings of the 2020 Optical fiber Communications Conference and Exhibition (OFC), IEEE, San Diego, CA, USA, 8–12 March 2020; pp. 1–3.
85. Zhou, Y.; Zhu, X.; Hu, F.; Shi, J.; Wang, F.; Zou, P.; Liu, J.; Jiang, F.; Chi, N. Common-anode LED on a Si substrate for beyond 15 Gbit/s underwater visible light communication. *Photonics Res.* **2019**, *7*, 1019–1029. [CrossRef]
86. Chen, Y.; Kong, M.; Ali, T.; Wang, J.; Sarwar, R.; Han, J.; Guo, C.; Sun, B.; Deng, N.; Xu, J. 26 m/5.5 Gbps air-water optical wireless communication based on an OFDM-modulated 520-nm laser diode. *Opt. Express* **2017**, *25*, 14760–14765. [CrossRef] [PubMed]
87. Liu, X.; Yi, S.; Zhou, X.; Fang, Z.; Qiu, Z.J.; Hu, L.; Cong, C.; Zheng, L.; Liu, R.; Tian, P. 34.5 m underwater optical wireless communication with 2.70 Gbps data rate based on a green laser diode with NRZ-OOK modulation. *Opt. Express* **2017**, *25*, 27937–27947. [CrossRef] [PubMed]
88. Tsai, C.L.; Lu, Y.C.; Yu, C.M.; Chen, Y.J. Epitaxial growth of InGaN multiple-quantum-well LEDs with improved characteristics and their application in underwater optical wireless communications. *IEEE Trans. Electron Devices* **2018**, *65*, 4346–4352. [CrossRef]
89. Cossu, G.; Sturniolo, A.; Messa, A.; Scaradozzi, D.; Ciaramella, E. Full-fledged 10Base-T ethernet underwater optical wireless communication system. *IEEE J. Sel. Areas Commun.* **2017**, *36*, 194–202. [CrossRef]
90. Liu, T.; Zhang, H.; Zhang, Y.; Song, J. Experimental demonstration of LED based underwater wireless optical communication. In Proceedings of the 2017 4th International Conference on Information Science and Control Engineering (ICISCE), IEEE, Changsha, China, 21–23 July 2017; pp. 1501–1504.
91. Hamza, T.; Khalighi, M.A.; Bourennane, S.; Léon, P.; Opderbecke, J. Investigation of solar noise impact on the performance of underwater wireless optical communication links. *Opt. Express* **2016**, *24*, 25832–25845. [CrossRef]
92. Xing, F.; Yin, H. Performance Analysis for Underwater Cooperative Optical Wireless Communications in the Presence of Solar Radiation Noise. In Proceedings of the 2019 IEEE International Conference on Signal Processing, Communications and Computing (ICSPCC), IEEE, Dalian, China, 20–22 September 2019; pp. 1–6.
93. Xing, F.; Yin, H.; Ji, X.; Leung, V.C.M. Joint Relay Selection and Power Allocation for Underwater Cooperative Optical Wireless Networks. *IEEE Trans. Wirel. Commun.* **2020**, *19*, 251–264. [CrossRef]
94. Alley, D.; Mullen, L.; Laux, A. Compact, dual-wavelength, non-line-of-sight (nlos) underwater imager. In Proceedings of the OCEANS'11 MTS/IEEE KONA, IEEE, Waikoloa, HI, USA, 19–22 September 2011; pp. 1–5.
95. Sun, X.; Kong, M.; Alkhazragi, O.; Shen, C.; Ooi, E.N.; Zhang, X.; Buttner, U.; Ng, T.K.; Ooi, B.S. Non-line-of-sight methodology for high-speed wireless optical communication in highly turbid water. *Opt. Commun.* **2020**, *461*, 125264. [CrossRef]
96. Sun, X.; Cai, W.; Alkhazragi, O.; Ooi, E.N.; He, H.; Chaaban, A.; Shen, C.; Oubei, H.M.; Khan, M.Z.M.; Ng, T.K.; et al. 375-nm ultraviolet-laser based non-line-of-sight underwater optical communication. *Opt. Express* **2018**, *26*, 12870–12877. [CrossRef]
97. Haltrin, V.I. One-parameter two-term Henyey-Greenstein phase function for light scattering in seawater. *Appl. Opt.* **2002**, *41*, 1022–1028. [CrossRef]
98. Toublanc, D. Henyey–Greenstein and Mie phase functions in Monte Carlo radiative transfer computations. *Appl. Opt.* **1996**, *35*, 3270–3274. [CrossRef] [PubMed]
99. Gabriel, C.; Khalighi, M.A.; Bourennane, S.; Léon, P.; Rigaud, V. Monte-Carlo-based channel characterization for underwater optical communication systems. *J. Opt. Commun. Netw.* **2013**, *5*, 1–12. [CrossRef]
100. Nguyen, H.; Choi, J.H.; Kang, M.; Ghassemlooy, Z.; Kim, D.; Lim, S.K.; Kang, T.G.; Lee, C.G. A MATLAB-based simulation program for indoor visible light communication system. In Proceedings of the 2010 7th International Symposium on Communication Systems, Networks & Digital Signal Processing (CSNDSP 2010), IEEE, Newcastle Upon Tyne, UK, 21–23 July 2010; pp. 537–541.
101. Fang, C.; Li, S.; Wang, K. Investigation of wavy surface impact on non-line-of-sight underwater optical wireless communication. In Proceedings of the 2022 IEEE Photonics Conference (IPC), IEEE, Vancouver, BC, Canada, 13–17 November 2022; pp. 1–2.
102. Tao, L.; Hongming, Z.; Jian, S. Distribution of Arriving Angle of Signal in Underwater Scattering Channel. *Chin. J. Lasers* **2018**, *45*, 306003.
103. Jaruwatanadilok, S. Underwater Wireless Optical Communication Channel Modeling and Performance Evaluation using Vector Radiative Transfer Theory. *IEEE J. Sel. Areas Commun.* **2008**, *26*, 1620–1627. [CrossRef]
104. Sait, M.; Trichili, A.; Alkhazragi, O.; Alshaibaini, S.; Ng, T.K.; Alouini, M.S.; Ooi, B.S. Dual-wavelength luminescent fibers receiver for wide field-of-view, Gb/s underwater optical wireless communication. *Opt. Express* **2021**, *29*, 38014–38026. [CrossRef]
105. Chen, J.; Jiang, M. Joint Blind Channel Estimation, Channel Equalization, and Data Detection for Underwater Visible Light Communication Systems. *IEEE Wirel. Commun. Lett.* **2021**, *10*, 2664–2668. [CrossRef]
106. Li, Y.; Liang, H.; Gao, C.; Miao, M.; Li, X. Temporal dispersion compensation for turbid underwater optical wireless communication links. *Opt. Commun.* **2019**, *435*, 355–361. [CrossRef]
107. Mahmutoglu, Y.; Turk, K.; Tugcu, E. Particle swarm optimization algorithm based decision feedback equalizer for underwater acoustic communication. In Proceedings of the 2016 39th International Conference on Telecommunications and Signal Processing (TSP), IEEE, Vienna, Austria, 27–29 June 2016; pp. 153–156.

108. Pinho, V.M.; Chaves, R.S.; Campos, M.L. On Equalization Performance in Underwater Acoustic Communication. In Proceedings of the XXXVI Simpósio Brasileiro de Telecomunicaçoes e Processamento de Sinais, SBrT, Campina Grande, Brazil, 16–19 September 2018.
109. Song, H. Bidirectional equalization for underwater acoustic communication. *J. Acoust. Soc. Am.* **2012**, *131*, EL342–EL347. [CrossRef] [PubMed]
110. Xie, Y.; Wang, Y.; Kandeepan, S.; Wang, K. Machine learning applications for short reach optical communication. *Photonics* **2022**, *9*, 30. [CrossRef]
111. Zhao, Y.; Zou, P.; Chi, N. 3.2 Gbps underwater visible light communication system utilizing dual-branch multi-layer perceptron based post-equalizer. *Opt. Commun.* **2020**, *460*, 125197. [CrossRef]
112. Chen, H.; Zhao, Y.; Hu, F.; Chi, N. Nonlinear resilient learning method based on joint time-frequency image analysis in underwater visible light communication. *IEEE Photonics J.* **2020**, *12*, 1–10. [CrossRef]
113. Chen, H.; Niu, W.; Zhao, Y.; Zhang, J.; Chi, N.; Li, Z. Adaptive deep-learning equalizer based on constellation partitioning scheme with reduced computational complexity in UVLC system. *Opt. Express* **2021**, *29*, 21773–21782. [CrossRef]
114. Zhao, Y.; Yu, S.; Chi, N. Transfer Learning–Based Artificial Neural Networks Post-Equalizers for Underwater Visible Light Communication. *Front. Commun. Netw.* **2021**, *2*, 658330. [CrossRef]
115. Du, Z.; Ge, W.; Cai, C.; Wang, H.; Song, G.; Xiong, J.; Li, Y.; Zhang, Z.; Xu, J. 90-m/660-Mbps Underwater Wireless Optical Communication Enabled by Interleaved Single-Carrier FDM Scheme Combined with Sparse Weight-Initiated DNN Equalizer. *J. Light. Technol.* **2023**. [CrossRef]
116. Cui, X.; Yin, X.; Chang, H.; Liao, H.; Chen, X.; Xin, X.; Wang, Y. Experimental study of machine-learning-based orbital angular momentum shift keying decoders in optical underwater channels. *Opt. Commun.* **2019**, *452*, 116–123. [CrossRef]
117. Avramov-Zamurovic, S.; Nelson, C.; Esposito, J.M. Effects of underwater optical turbulence on light carrying orbital angular momentum and its classification using machine learning. *J. Mod. Opt.* **2021**, *68*, 1041–1053. [CrossRef]
118. Romdhane, I.; Kaddoum, G. A Reinforcement-Learning-Based Beam Adaptation for Underwater Optical Wireless Communications. *IEEE Internet Things J.* **2022**, *9*, 20270–20281. [CrossRef]
119. Weng, Y.; Pajarinen, J.; Akrour, R.; Matsuda, T.; Peters, J.; Maki, T. Reinforcement learning based underwater wireless optical communication alignment for autonomous underwater vehicles. *IEEE J. Ocean. Eng.* **2022**, *47*, 1231–1245. [CrossRef]
120. Wang, J.; Luo, H.; Ruby, R.; Liu, J.; Guo, K.; Wu, K. Reliable Water-Air Direct Wireless Communication: Kalman Filter-Assisted Deep Reinforcement Learning Approach. In Proceedings of the 2022 IEEE 47th Conference on Local Computer Networks (LCN), IEEE, Edmonton, AB, Canada, 26–29 September 2022; pp. 233–238.
121. Li, X.; Hu, X.; Li, W.; Hu, H. A multi-agent reinforcement learning routing protocol for underwater optical sensor networks. In Proceedings of the ICC 2019-2019 IEEE International Conference on Communications (ICC), IEEE, Shanghai, China, 20–24 May 2019; pp. 1–7.
122. Li, X.; Hu, X.; Zhang, R.; Yang, L. Routing protocol design for underwater optical wireless sensor networks: A multiagent reinforcement learning approach. *IEEE Internet Things J.* **2020**, *7*, 9805–9818. [CrossRef]
123. Khalighi, M.; Akhouayri, H.; Hranilovic, S. SiPM-based Underwater Wireless Optical Communication Using Pulse-Amplitude Modulation. *IEEE J. Ocean. Eng.* **2020**, *45*, 1611–1621. [CrossRef]
124. Li, C.; Wang, B.; Wang, P.; Xu, Z.; Yang, Q.; Yu, S. Generation and transmission of 745 Mb/s ofdm signal using a single commercial blue LED and an analog post-equalizer for underwater optical wireless communications. In Proceedings of the 2016 Asia Communications and Photonics Conference (ACP), IEEE, Wuhan, China, 2–5 November 2016; pp. 1–3.
125. Cheng, C.; Li, X.; Yang, Y. Net 4.12 Gb/s UOWC System over 2 m Using a Single-Pixel Blue Mini-LED and a Simplified Third-Order Volterra Equalizer. In Signal Processing in Photonic Communications; Optica Publishing Group: Maastricht, The Netherlands, 2022; p. SpTh3H–5.
126. Yu, M.; Geldard, C.T.; Popoola, W.O. Comparison of CAP and OFDM Modulation for LED-based Underwater Optical Wireless Communications. In Proceedings of the 2022 International Conference on Broadband Communications for Next Generation Networks and Multimedia Applications (CoBCom), IEEE, Graz, Austria, 12–14 July 2022; pp. 1–6.
127. Yang, H.; Yan, Q.; Wang, M.; Wang, Y.; Li, P.; Wang, W. Synchronous Clock Recovery of Photon-Counting Underwater Optical Wireless Communication Based on Deep Learning. *Photonics* **2022**, *9*, 884. [CrossRef]
128. Chi, N.; Jia, J.; Hu, F.; Zhao, Y.; Zou, P. Challenges and prospects of machine learning in visible light communication. *J. Commun. Inf. Netw.* **2020**, *5*, 302–309. [CrossRef]
129. Xu, Z.; Chen, T.; Qin, G.; Chi, N. Applications of Machine Learning in Visible Light Communication. In Proceedings of the 2021 18th China International Forum on Solid State Lighting & 2021 7th International Forum on Wide Bandgap Semiconductors (SSLChina: IFWS), IEEE, Shenzhen, China, 6–8 December 2021; pp. 198–201.